Mechanism of Microgel Formation via Cross-Linking of Polymers in Their Dilute Solutions: Mathematical Explanation with Computer Simulations

Kenneth S. Schmitz*

Department of Chemistry, University of Missouri—Kansas City, Kansas City, Missouri 64110

Benlian Wang and Etsuo Kokufuta

Institute of Applied Biochemistry, University of Tsukuba, Tsukuba, Ibaraki 305, Japan

Received June 1, 2001; Revised Manuscript Received September 6, 2001

ABSTRACT: The formation of poly(vinyl alcohol) microgels by γ-ray irradiation was previously studied by static and dynamic light scattering methods to obtain respectively the radius of gyration (R_g) and the hydrodynamic radius (R_h). It was proposed that the mechanism of this microgel formation was an intermolecular cross-linking step followed by an intramolecular cross-linking process. Presented herein is a mathematical model for interpreting the values of R_g and R_h, in which the Kirkwood theory of the friction factor was employed. To mimic the known extensions of "brushes", a set of "bias parameters" were employed for the purpose of making a directional preference in generating the configurations of both parent and branch chains. The simulations with this simple model are in very good agreement with the proposed mechanism of microgel formation in the poly(vinyl alcohol) system. Justification of using the "bias parameters" is supported by computationally intensive Brownian dynamics simulations of a collection of 216 "beads" with a "Velcro" pair potential, i.e., a short-range "attractive" pair potential that acts as a formation of a chemical bond between the beads. The advantage of the "bias" walk model is that it allows one to explore different molecular configurations on a smaller computer and thus to select an appropriate set of parameters for more extended and time-consuming simulations on mainframe computers.

1. Introduction

Cross-linked polymer networks with nanometer sizes, i.e., microgel particles, are of interest in both scientific and technical fields.[1−21] Many studies[1−16] have focused on microgels that undergo an abrupt size change in response to alterations in solution conditions such as temperature and pH. The microgels of this sort were prepared via polymerization or copolymerizations of a well-known thermosensitive monomer, *N*-isoproplyacrylamide (NIPA), using a cross-linking agent such as *N*,*N*′-methylenebis(acrylamide).

In the preparation of microgels, on the other hand, polymers but not monomers have been employed by a combination with suitable cross-linking techniques. A good example for this is γ-ray irradiation to solution of poly(vinyl alcohol) (PVA).[17−21] Since PVA has good biocompatibility,[22] much attention has been paid to the formation of its hydrogels, in the forms of both microgels[17−21] and bulk gels.[23−32] There is a limiting irradiation dose, i.e., gelation dose (D_g), at which the gel formation sets in. At doses $> D_g$, the irradiation yields either a bulk gel or microgel particles depending on the polymer concentration (C_p). Thus, this characteristic concentration is often referred to as the critical polymer concentration (C_{pc}); the microgel formation takes place at $C_p < C_{pc}$, whereas at $C_p > C_{pc}$ the bulk gel forms. Both D_g and C_{pc} depend on the molecular weight (M_w) of the polymer.

There are two types of cross-linking processes,[20,21,31,32] that is, *inter*- and *intra*polymer cross-linking. The former allows the increase of the molecular weight (M_w) of a cross-linked polymer via the coupling of two or more polymer chains. The latter does not alter M_w but affects the quantities relating to a polymer chain dimension, e.g., hydrodynamic radius (R_h) as well as radius gyration (R_g), because the cross-linking should take place within the same polymer chain. Indeed, Brasch and Burchard[19] employed static and dynamic laser light-scattering techniques in their study of PVA microgels, which were prepared through chemical cross-linking with glutaraldehyde.

Previous studies on PVA microgel formation by γ-rays employed static and dynamic light scattering techniques to monitor the progress of the reaction.[10] Static light scattering data provided information on the molecular weight (M_w) from total intensity measurements and the radius of gyration (R_g) from the angle dependence of the total intensity. Dynamic light scattering provided values of the hydrodynamic radius (R_h). These parameters were obtained as a function of C_p and irradiation dose.[20] A mechanism was proposed in which intermolecular cross-linking first occurred, which was then followed by intramolecular cross-linking to a more compact structure.

The objectives of the present study are twofold. The first objective is to provide quantitative support for the proposed mechanism as reflected in the ratio R_g/R_h. The second objective is to devise a mathematical model that is simple enough to carry out the calculations on a PC since more elaborate simulations on a mainframe computer can be very time intensive. To achieve the latter objective, a modification of the Kirkwood bead model is proposed, that of "bias" steps in the generation of the "random" structures. Thus, from these "exploratory" investigations one may chose optimal parameters to use in more sophisticated simulations. Justification for the "bias" model is supported by Brownian dynamics simulations with a "Velcro" potential.

10.1021/ma010956+ CCC: $20.00
Published on Web 10/12/2001

2. The Kirkwood Model

In principle, R_g and R_h can be calculated quite accurately with the powerful theories that exist at this time if the distribution of mass and the friction centers are accurately known. While such knowledge may be available for well-defined structures that are ubiquitous in biological systems, such as the viruses, a similar situation does not exist for randomly generated structures such as the microgels in the present study. Therefore, we resort to the most primitive of hydrodynamic theories, the subunit model of Kirkwood for polymers of arbitrary shape,[33] that still permits one to extract useful information regarding the statistical nature of equivalent hydrodynamic structures. The effective hydrodynamic radius of the polymer is calculated from the Kirkwood prescription

$$R_h = \frac{n_s r_s}{1 + \frac{r_s}{n_s}\sum_{j=1}^{n_s}\sum_{i=1>\neq j}^{n_s}\frac{1}{r_{ij}}} \tag{1}$$

where n_s is the number of subunits in the microgel, r_s is the radius of the equivalent sphere for the point friction source, and r_{ij} is the spatial distance between the jth and ith subunit. The radius of gyration is calculated in the standard way for the arbitrary distribution of mass points,

$$R_g = \langle R_g^2\rangle^{1/2} = \left\langle \frac{1}{n_s}\sum_{j=1}^{n_s} R_j^2 \right\rangle^{1/2} \tag{2}$$

where it is assumed that each friction point has the same mass and the vector distance $\mathbf{R}_j$ is measured from the center-of-mass of the polymer. Thus, if the point sources of friction are also the point source for light scattering, then eqs 1 and 2 may be combined to calculate the ratio R_g/R_h, which is compared to the experimentally determined ratio.

3. Generation of the Cross-Linked Strands and Microgel Structures

The generation of a microgel is assumed to take place through inter- and intrachain cross-linking. The resulting structures are assumed to be "brushlike" in the sense that the envelop appears elongated with extended branches along a backbone. Direct application of the prescriptions of the Kirkwood theory results in a more compact, spherical array of friction beads. Therefore, to generate the more extended structure, a form of "bias" must be incorporated into the generation of the friction chain.

It is well-known that excluded-volume effects act as a repulsive force between subunits and that the dimensions of the resulting random structure are larger than those of the random flight, or "phantom chain", calculations. To illustrate the effect of excluded volume, we have generated chains from monomer units uniformly distributed in a cubic lattice by Brownian dynamics (BD) methods. The detail of the simulations is given in the Appendix. To mimic the formation of chemical bonds, we employ a "Velcro" potential of the Yukawa form

$$\beta U_{pp} = -A\frac{\exp(-yr)}{r} \tag{3}$$

where $\beta = 1/k_BT$, k_B is the Boltzmann constant, T is the absolute temperature, A is a positive constant that measures the strength of the interaction, y is a constant that determines the rate of change of the interaction with distance, and r is a reduced distance given in units of the radius of the bead particles. To ensure a "strong chemical bond" acting over a short range, the values $A = 2.2 \times 10^9$ and $y = 7.34$ were used in the simulations. Shown in Figure 1 are the potential, the initial cubic array configuration of the 216 subunits, and the final configuration after 10^7 attempted moves for each subunit. The number of attempted moves, 10^7, is not an arbitrary number in this particular simulation. It represents the number of moves necessary to have no remaining monomer units, where the movement of particles was monitored after every 10^6 attempted moves. That is, after a "contact" has been made between two beads, the resulting "unit" does not move since the "Velcro" potential does not allow dissociation as would also be the case for chemical bonds. Hence, the structures shown in panel C of Figure 1 obtain from the addition of monomer units to preexisting clusters until no more monomer units remain in the system. The structures in panel C are highly extended. Because of the highly extended nature of these structures, one can define a pathway through contiguous beads that represents a "parent" chain from which the other beads, or branches, may be attached. All of our other simulations show similar structures of clustered units for a variety of choices of A and y with the constraint that the profile be sharp as shown in panel A of Figure 1. For example, those simulations with $\phi_p = 0.001$ give structures that are also extended but do not "grow" too far beyond trimers and tetramers since, once formed, the clusters themselves do not move. The simulations shown in Figure 1 were generated over a period of a few days and represent $3 \times 216 \times 10^7 = 6.48 \times 10^9$ attempted coordinate moves. To generate larger clusters that may mimic microgel formation would be prohibitive because of the necessary computer time.

In relationship to the experiment, the starting polymers may be assumed to be highly extended. As polymers are cross-linked together in the interchain process, the resulting structures may also be assumed highly extended, forming branched structures and possible looped regions. With this final configuration in mind one can choose a pathway through contiguous units that represents a "parent" chain from which the remaining units may be considered to be branches. It is this physical picture that we now generate mathematically as a two-step process using the Kirkwood bead model. To ensure that extended structures result from the Kirkwood model, we introduce "bias parameters" a, b, and c into our chain generation via the prescription

$$\mathbf{r}_{j+1} = \mathbf{r}_j + L_s(\mathrm{Ran1} - a, \mathrm{Ran2} - b, \mathrm{Ran3} - c) \tag{4}$$

where $\mathbf{r}_{j+1}$ is the location of the $j + 1$ bead when the step originates from the jth bead; Ran1, Ran2, and Ran3 are random real numbers between 0 and +2; and L_s is

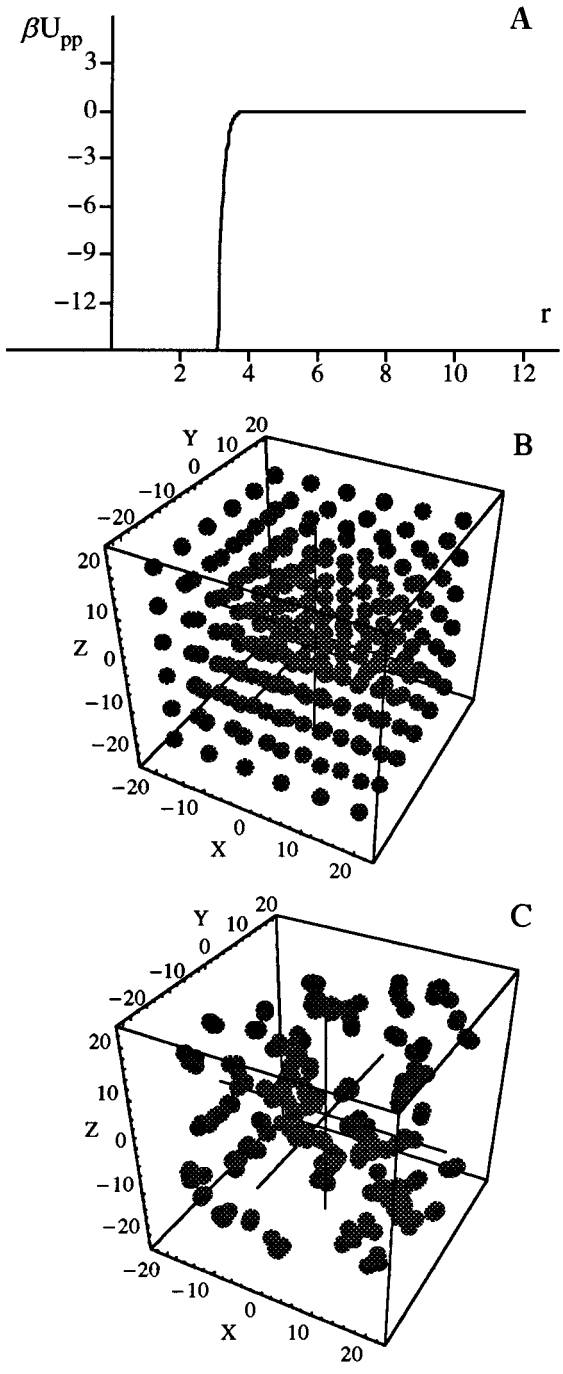

Figure 1. Brownian dynamics simulations of aggregation. The top figure is the pairwise attractive potential acting between two spheres, as defined by eq 3 and using the parameters $A = 2.2 \times 10^9$, $y = 7.34$, and $\phi_p = 0.01$. Part B is the initial cubic array for $N_p = 216$ spheres. Part C is the result of 10^7 attempted movements for each particle where the step size is $s = 0.1$.

the extension step size that reflects the degree of "stiffness" of the chain.

To understand what is meant by "bias", we first consider a chain that has no bias. Since the first unit of the parent chain is at the origin, the "forward" direction is defined as a positive displacement and the "backward" direction as a negative displacement. In this case a step forward is equally probable as a step backward. Hence, the sum Ran1 − a must have the range −1 to +1. Thus, the value $a = 1$ represents a completely random generation, and L_s is the maximum step length. On the other hand, the interaction between neighboring units is "directionally limited", such as might occur because of the bond angle, excluded-volume effects, or repulsive electrostatic interactions. That is, the probability of a step in the positive direction (forward direction) is larger than in the negative direction. As an example, consider first the value of 0.5 for the bias parameter. The maximum step in the forward direction along this coordinate is $1.5L_s$ whereas in the maximum backward step is $-0.5L_s$. Thus, there are two ways to influence the configuration of a generated chain: the overall extension of the configuration is controlled through the parameter L_s, and the directional asymmetry is controlled by varying the bias parameters a, b, and c.

The typical envelop of a brush structure is cylindrical in shape, viz., elongated in one direction that may define its "primary" axis and having a finite "thickness" that is defined by shorter structures with a bias along the other two axes. The configuration of the microgel in the present study was thus constructed in two steps to obtain a "brush structure": generation of a "parent chain" of n_p subunits with a bias in the z-direction and then generation of n_B "branch chains" of n_b subunits, each with biases in the x and y directions. This "brush structure" has a total of $n_s = n_P + n_B n_b$ subunits with the primary axis as being along the z-axis.

The parent and branch chains are generated separately with the stated bias direction(s). The location of the first bead in each of these generations is at the origin of the local coordinate system. The initial set of integers ranges from $1 \le I_p \le n_p$ for the parent chain and $1 \le I_b \le n_b$ for the branch chain. The "contact beads" are defined as the first bead in the branch chain, $I_b = 1$, and a randomly generated integer number for its location on the parent chain, I_r. Once chosen as a "contact site", the location $I_p = I_r$ on the parent chain is then removed from the pool of future contact sites. Having now established the contact beads of the parent and branch chains, in their local relative coordinates, we next move the branch chains to the parent chain. For example, if the cross-linking point is the jth location on the parent chain and the kth location on the branch chain, then the docking of the branch chain to the parent chain is effected by addition of the set of coordinates $\mathbf{P}(j) - \mathbf{B}(k) + \mathbf{O}$ to each local coordinate of the branch chain. In this prescription $\mathbf{P}(j)$ is the set of coordinates for the jth location of the parent chain, $\mathbf{B}(k)$ is the set of local coordinates of the kth location of the branch chain, and $\mathbf{O}$ is a fixed set of coordinates of unit length to avoid overlap (contact) of the two friction points at the cross-linking locations. The vector $\mathbf{O}$ is determined by random number generation for each of the individual branch chains. It is noted that in this prescription only the contact beads are specifically generated as being in close proximity of each other. Any possible formation of loops and multiple contacts between any of the component chains is a consequence of the random nature of their generation and the subsequent docking of the branch chains.

Once the location of all the n_p and n_s beads have been established, the center-of-mass of the structure is located, and the respective bead coordinates are thus shifted to the center-of-mass coordinate system, viz., $\mathbf{R}_j = \mathbf{r}_j - \mathbf{R}_{com}$, where j runs over the set of locations n_s. A schematic representation of the docking construction of the microgel is given in Figure 2.

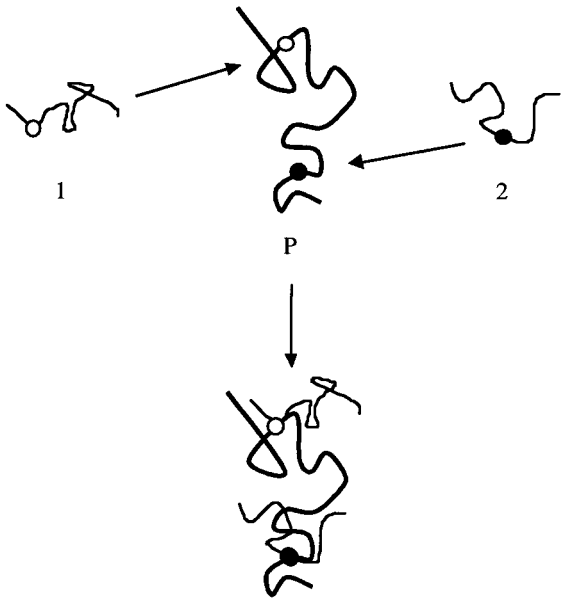

Figure 2. Schematic of the generation of microgel structures. Shown above is one "parent" chain, denoted by "P", and two branch chains. These chains were independently generated by the procedure outlined in the text. Once generated, the location of the sites for attachment are randomly determined. In the above case the attachment of chain 1 to P is indicated by the open circles (○) and of chain 2 to P by the closed circles (●). The two branch chains are then "docked" to the parent chain at these locations by translation motion. Not shown is the separation distance **O** for the two contact beads.

4. Characteristics of the Bias Chain Model: Computer Simulations

We now look at some of the characteristics of using "bias" in the calculations of the coil configuration. All of the calculations performed in this study were done with programs written in *Mathematica*, a means of doing mathematics on the computer.

We first establish reference configurations by which the extent of "bias" may affect our calculations. The random configuration defined by $a = b = c = 1$ is the obvious choice. Since the γ-ray irradiation may increase the molecular weight, the physical parameters R_g and R_h for the unbiased model were determined as a function of chain length by changing n_p and n_b by the same multiplicative factor but retaining the value of n_B. In Figure 3 are calculations for the random coil configurations with $n_p = 50$, $n_B = 10$, and $n_b = 15$ (configuration R1) and with $n_p = 200$, $n_B = 10$, and $n_b = 60$ (configuration R2). The calculated values of R_g and R_h are, in arbitrary units, 2.160 and 2.113, respectively, with the ratio $R_g/R_h = 1.022$ for R1 and 5.186 and 4.800, respectively, and with the ratio $R_g/R_h = 1.080$ for R2. Thus, the random generation of microgels provides a ratio R_g/R_h resembling that of a hollow sphere in which all of the mass is located at its surface rather than a solid sphere, which has the theoretical value $R_g/R_h = (3/5)^{1/2} = 0.77$.

We next look at a biased parent ($a = b = c = 0.5$) with unbiased branch chains. Conformation R3 is generated with $n_p = 50$, $n_B = 10$, and $n_b = 15$ and conformation R4 with $n_p = 50$, $n_B = 10$, and $n_b = 50$. Conformations R3 and R4 are shown in Figure 4. The calculated values of R_g and R_h for the biased parents are 11.953 and 6.228, respectively, with the ratio $R_g/R_h = 1.919$ for R3, and for R4 the values are 15.994 and 8.981, respectively, with the ratio $R_g/R_h = 1.781$. It is of interest to note that the individual values of R_g and R_h increase in going from R3 to R4, as they should with an increase in the molecular weight of the branches. However, the ratio R_g/R_h decreases with the increase in the molecular weight due to the fact the *relative* bias of complexed chain has changed. This comparison again supports the notion that the ratio R_g/R_h is a good measure of conformational changes in the chains.

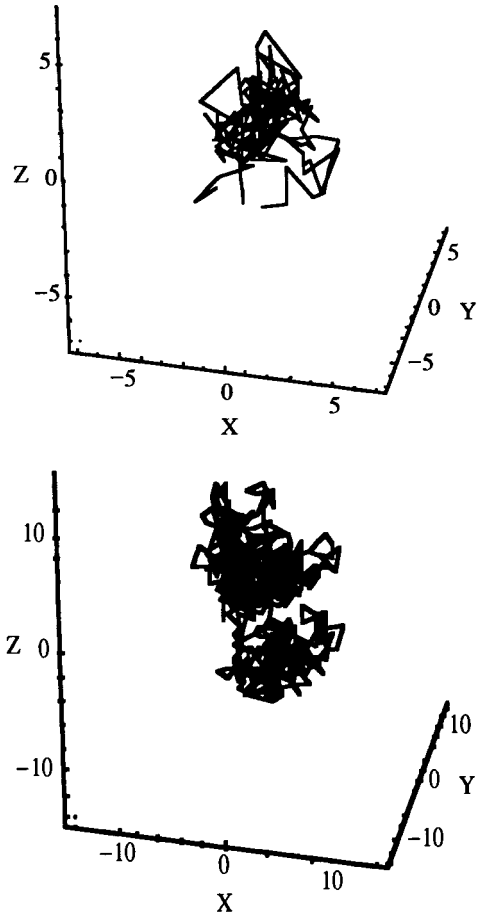

Figure 3. Random coil structures. The above structures were generated for the random coil structure; i.e., the bias parameters were $a = b = c = 1$. (top) The number of subunits in the parent was $n_p = 50$ and for the $n_B = 10$ branch chains with $n_b = 15$. The calculated values of R_g and R_h are 2.160 and 2.113, respectively, in arbitrary units, with the ratio $R_g/R_h = 1.022$. (bottom) The number of units in the parent chain of $n_p = 200$ and number of branch chains $n_B = 10$ of length $n_b = 60$. The calculated values of R_g and R_h are 5.186 and 4.800, respectively, with the ratio $R_g/R_h = 1.080$.

5. Application of the Model to Data on Microgels

Table 1 shows the experimental data of dynamic and static light scattering for the formation of the microgels from aqueous O_2-free solutions of PVA ($M_w = 1 \times 10^5$ g/mol as the original) by means of γ-ray irradiation. The data were obtained in our previous study,[20] in which more data were reported on the formation of bulk PVA gels. However, we focus only on the experiments performed at the PVA concentrations = 2.0 and 1.6 g/L, which are considered as these lie below the C_{pc} (critical polymer concentration). Data analysis in the semidilute concentration regime (i.e., $> C_{pc}$) are governed by equations not considered in the present analysis and hence lie outside the domain of the present text. The reason

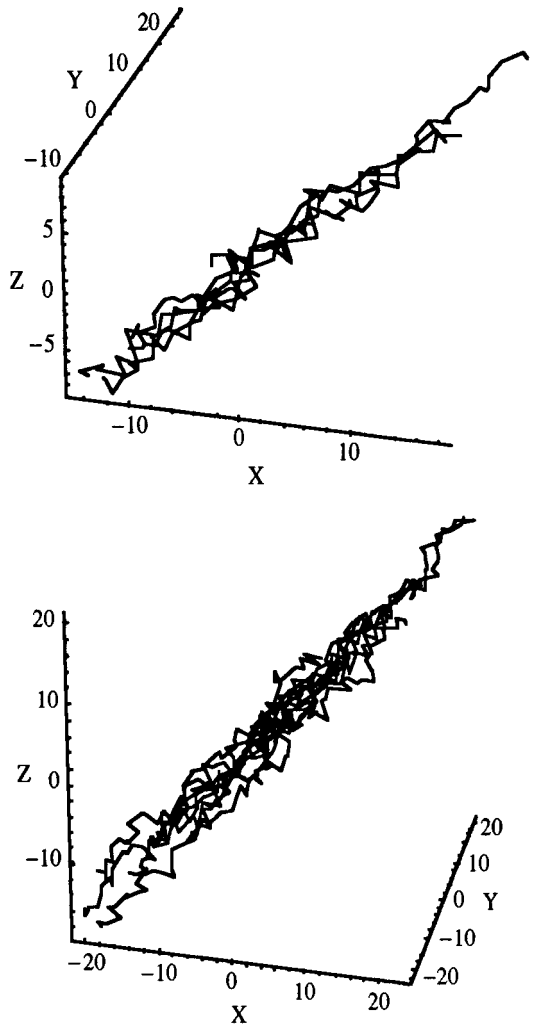

Figure 4. Biased parent, random coil branch structure. The above chains were generated for the bias parameters $a = b = c = 0.5$ for the parent and $a = b = c = 1$ for the branch chains. (top) The number of subunits in the parent was $n_p = 50$ and for the $n_B = 10$ branch chains with $n_b = 15$. The calculated values of R_g and R_h are 11.953 and 6.228, respectively, with the ratio $R_g/R_h = 1.919$. (bottom) The number of subunits in the parent was $n_p = 50$ and for the $n_B = 10$ branch chains with $n_b = 50$. The calculated values of R_g and R_h are 15.994 and 8.981, respectively, with the ratio $R_g/R_h = 1.781$.

Table 1. Light Scattering Data for Microgel Formation from Aqueous PVA Solutions by γ-ray Irradiation[a]

	irradiation conditions					
expt no.	concn (gL^{-1})	dose (Mrad)	M_w (10^5 g mol^{-1})	R_g (nm)	R_h (nm)	R_g/R_h
1		0	1.00[b]	17[b]	11[b]	1.52[b]
2	2.0	0.041	1.53	37	23	1.60
3	2.0	0.082	3.45	50	33	1.54
4	2.0	0.15	88.9	127	88	1.44
5	2.0	0.30	711	206	187	1.10
6	2.0	0.60	1040	202	184	1.10
7	2.0	1.20	1490	192	195	0.98
8	1.6	0.082	75.5	113	70	1.61
9	1.6	0.30	272	140	90	1.59
10	1.6	0.45	543	144	99	1.45
11	1.6	0.60	622	128	99	1.29
12	1.6	0.75	790	117	99	1.18

[a] All the data were obtained in our previous study (see Table 1 in ref 20). [b] Data at dose = 0 denote the original PVA before γ-ray irradiation.

for this is that the γ-ray irradiation at PVA concentrations $> C_{pc}$ led to the formation of bulk gels, whereas the present interest is on the structure and properties of the microgels.

We now focus attention to the experimental data, which may be partitioned into two groups in accordance with the value of the ratio R_g/R_h: (1) group 1 consists of microgel structures for which $R_g/R_h < 1.2$, and (2) group 2 are the structures for which $1.2 < R_g/R_h < 2.0$.

Within the stated definitions of the above two groups, the results from experiments 5−7 in Table 1 are group 1 occupants. It is significant that these are the highest molecular weights in the irradiated samples. As the molecular weight increases, one would expect the "local character" of the structure to be lost, and the structure becomes more like a random generated structure.

Attention is now directed to the concentrations of 1.6 g/L for experiments 8−12. All of these data may be included in group 2. Although the inclusion of experiment 12 as a group 2 occupant may be considered as marginal, its inclusion does emphasize a trend. Again, one can discern the trend to the more random structure as the molecular weight increases.

The proposed model for the experimental data is composed of two steps. The first step is the *interchain* cross-linking which results in an extended branch structure. The second stage is an *intrachain* cross-linking in which the structure undergoes a collapse in such a manner as to reduce the radius of gyration while maintaining an almost constant hydrodynamic radius. Physically, this means that the interior of the structure becomes more dense in scattering centers, thus reducing the value of R_g, while the exterior "hairs" of the structure become more extended such as to counteract the interior collapse contribution to the hydrodynamic properties of the microgel.

We undergo to test this mechanism in the following manner using bias generation of the parent and branch chains. We consider first the branched structure that results in the first step of the mechanism. An extended structure that may physically result from excluded-volume effects, thus a bias for the parent chain, is directed along the z-axis and the branch chains in the $x-y$ plane. This is effected by the set of bias parameters $a = b = 1$ and $c = 0.5$ for the parent chain and $a = b = 0.5$ and $c = 1$ for the branch chains. We use the value $n_p = 150$, $n_B = 10$, and $n_b = 45$ to compare with the calculations in Figure 2 for an increase in molecular weight by a factor of 3. The resulting structure, shown in Figure 5, gives values of $R_g = 37.278$ and $R_h = 19.618$ for a ratio of $R_g/R_h = 1.900$. In the second step of the proposed mechanism, the internal structure of the branched chain collapses due to *intra*molecular cross-linking. This collapse is effected in the simulations by changing the set of bias parameters for the parent strand to $a = b = c = 0.9$ and for the branch strands $a = b = c = 1$, with the step length set at $L_s = 0.8$ in both cases. The structure that was generated is shown in Figure 6, where the characteristic parameters now have the values of $R_g = 7.664$ and $R_h = 5.616$ for a ratio of $R_g/R_h = 1.365$. Note that in this case the value of R_g is less than that for the cross-linked structure in the top of Figure 4 (7.664 vs 11.953 or a 55% increase), but the value of R_h is virtually unchanged (5.616 vs 6.228, or an 11% increase) even though the molecular weight has increased by a factor of 3. Since the friction points are connected in the order in which they were generated, it is possible that the proximity of a group of points may be interpreted as the formation of rings or cyclic

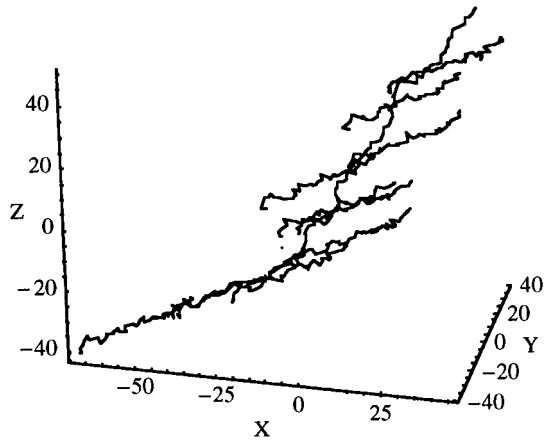

Figure 5. Structure of branched polymer for step 1 of mechanism: interchain cross-linking. In the first step of the mechanism there is extensive interchain cross-linking which results in an extended structure. The parent chain by setting its bias parameters to $a = b = c = 0.5$ and the branch chains with $a = b = c = 1$. In both cases $L_s = 1$. The number of subunits in the parent was $n_p = 150$ and for the $n_B = 10$ branch chains with $n_b = 45$. The calculated values of R_g and R_h are 37.278 and 19.618, respectively, with the ratio $R_g/R_h = 1.900$.

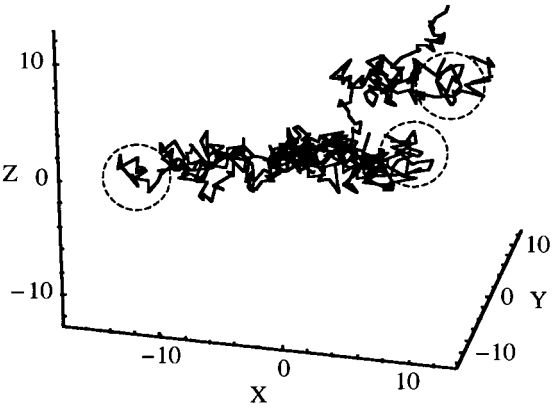

Figure 6. Structure of branched polymer for step 2 of mechanism: intrachain cross-linking with molecular weight increase. In the second step of the mechanism there is extensive intrachain cross-linking which results in a collapse of these chains. The parent chain by setting its bias parameters to $a = b = c = 0.9$ and the branch chains with $a = b = c = 1$. In both cases $L_s = 0.8$. The number of subunits in the parent was $n_p = 150$ and for the $n_B = 10$ branch chains with $n_b = 45$. The calculated values of R_g and R_h are 7.664 and 5.616, respectively, with the ratio $R_g/R_h = 1.365$. The dashed circles indicate regions in which a cyclic structure may be formed due to the proximity of the friction units.

structures. The dashed circles in Figure 6 indicate regions that may be interpreted as the formation of closed rings.

6. Discussion

Dynamic and static light-scattering studies[20,21] have led to a suggested mechanism of γ-ray-induced formation of PVA microgels at the molecular level. At the initial stage of the irradiation, the chain branching should take place via interpolymer cross-linking, regardless of polymer concentrations. Further interpolymer cross-linking allows for the resulting branched polymer to combine one another, through which both mass and size should be increased. When once a branched polymer is formed, the irradiation causes the intrapolymer cross-linking at the same time. If the polymer concentration is lower than C_{pc}, these simultaneously occurring intra- and interpolymer processes result in a microgel particle. Then we observed the following characteristics in the changes in R_h, R_g, and M_w as a function of irradiation dose. At the early stage of the irradiation, M_w as well as R_h and R_g increased rapidly. Upon further irradiation, M_w increased almost linearly, but R_h leveled off and R_g decreased. These results were explained in terms of structural change in the microgel particle, which was then assumed to have an obscure surface covering with dangling chain hairs at the early stage of the formation, then turning it into a "soft sphere" with a distinct surface. Such a model was originally proposed by Brasch and Burchard[19] in their study on chemically induced formation of PVA microgels. Although there was the striking resemblance in the microgel formation by the γ-ray and the chemically induced cross-linking, the model has not yet been examined in a quantitative and mathematical way.

We have proposed a mathematical approach to the study of the formation of microgels and applied it to the hydrodynamic characterization of γ-ray-irradiated PVA. Since the main objective was to testify to the validity of the interpretation of the values of the R_g/R_h ratio under variable experimental conditions, we employed a modification of the primitive Kirkwood model. The Kirkwood model represents a first-order correction to the friction factor of a chain composed of equal sized beads with friction sources solely at the center of the beads. Bloomfield and co-workers[34−36] attempted to correct for the fact that the friction source is not at the center of the bead but at the surface of the bead. In this regard higher order correction terms in the bead radius become important for contiguous beads of approximately the same size. However, if the bead separation is larger than the bead radius, then the Kirkwood formula gives better results.[36] This is due to the observation that the higher order correction terms are of alternating sign and may result in mutual cancellation. The error resulting from use of the Kirkwood expression is dependent upon the structure under examination. One problem is obtaining a theoretical standard that is the exact expression for the structure under consideration. One such structure is the prolate ellipsoid given by Perrin's expression,

$$f_{\text{prolate}} = \frac{6\pi\eta b(1-p^2)^{1/2}}{\ln\left[\dfrac{1+(1-p^2)^{1/2}}{p}\right]} \qquad (5)$$

where $p = b/a$ is the ratio of the semiminor (b) and semimajor (a) axis. Bloomfield et al.[34] used Perrin's exact expression for a prolate ellipsoid as a reference. They concluded that the Kirkwood expression gave the correct asymptotic approach in the limit $a/b \rightarrow \infty$. The present focus is on flexible chains, where internal motions are coupled which might affect the calculation of the friction properties of the molecule. In this case Monte Carlo simulations may be assumed to represent the theoretical standard. Although somewhat related to the present system, Zimm[37] compared the hydrodynamics of a chain with Gaussian distributed segments in Monte Carlo simulations with the predictions of the Kirkwood−Riseman theory of the sedimentation coefficient and intrinsic viscosity. This comparison showed about a 15% error as compared to the MC simulations. Similar studies with wormlike star molecules[38] indicate that the difference between experimental measurements

and the commonly used formulas are due partly to preaveraging and chain extension because of chain stiffness and mutual repulsion of the chains emanating from the branch point. The latter effect, mutual repulsion of chains from the branch point, is represented in the present situation by the bias parameters, in the *z* direction for the parent chain and the *x* and *y* directions for the branches. It may be concluded that the error for very long chains with bias as employed in our simulations is of no consequence for the stated objective of explaining the experimental observations within the bounds of reasonable computation time and programming simplicity.

The modification we employed is a set of "bias parameters" for directional preference in generating the "extended random coil" configurations of both parent and branch chains that one might expect for a gel network system due to intermolecular cross-linking, with the possibility of including the effects of intramolecular cross-linking to contract the network to microgels. As a means of justification of the use of "bias" parameters, we employed Brownian dynamics simulation methods to generate a "chain" from random movement of monomer units using a "Velcro" potential. As noted by Zimm,[38] chain exclusion due to mutual repulsion in star molecules likewise results in a more extended structure at the branch points.

For the truly random walk linear polymer the chain length dependence of R_g takes on the power law $R_g = KM^{0.5}$, where K is a constant. From the calculations associated with Figure 2 we obtain from the relationship between the ratios $(4/1)^d = (5.186/2.160)$, the power law $d = 0.63$. The difference in the two power laws, at this level of approximation, is attributed to the requirement of contact points between the branch chains and the parent chain rather than the random number method of generating the chains. By placing the branch chains along the parent chain, the structure approaches that of a cylinder in shape, and we would expect $d > 0.5$. In contrast, if the branch chains were all placed at the same location of the parent chain, then the structure would approach that of a sphere as in the generation of "star" structures, and we would expect $d < 0.5$.

When PVA aqueous solution is suffered to γ-ray irradiation, small branched polymers are formed via intermolecular cross-linking at the initial stage, regardless of the polymer concentration. At concentrations $< C_{pc}$, the combination of the small branched polymers takes place to result in a larger branched polymer. After that, the intrapolymer cross-linking within the branched polymer results in a microgel particle. This process accompanies phase separation, and solution turbidity appears. However, if a microgel with an obscure surface due to several dangling chains is initially formed, then such microgels combine with several branched polymers to increase M_w. Since the intramolecular cross-linking simultaneously takes place at this stage, there is little increase in the size but a rise in the segment density. As a result, the microgel gradually turns into a "soft sphere" with a distinct surface. The calculations given in Figures 4−6 reflect this behavior. The data in Figure 4 is used as a reference structure, with of $R_g = 11.953$ and $R_h = 6.228$, for a ratio $R_g/R_h = 1.919$. Intermolecular cross-linking give the structure represented in Figure 6, where the molecular weight is increased by a factor of 3. This increase in molecular weight without a change in the parameters for the generation of the conformation yield values of $R_g = 37.278$ and $R_h = 19.618$, for a ratio $R_g/R_h = 1.900$. The apparent constancy of R_g/R_h in the vicinity of 1.9 supports the notion that the general nature of the chain is unchanged with the increase in the molecular weight. The step 2 process, involving only intramolecular cross-linking, does give rise to a change in the nature of the chain. As shown in Figure 6, the conformation that corresponds to a "collapse" is characterized by the values of $R_g = 7.664$ and $R_h = 5.616$, for a ratio $R_g/R_h = 1.365$. Note that the values of R_h for the "monomer unit" (Figure 4 structure) and the "microgel unit" (Figure 6 structure) are comparable in value while there is a significant difference in the R_g values.

We conclude that the mechanism proposed for the microgel formation as an interchain cross-linking process followed by an intrachain cross-linking to a more collapsed structure is accurately portrayed by the "bias walk" model as proposed. These simulations of a simultaneous collapse of the interior structure due to intramolecular cross-linking with an increase in the extension of the branch chains is thus a verification of the model proposed by Burchard and co-workers.[19] In addition, the "bias walk" model offers a viable approach to search for "candidate" structures for the more time intensive computations with more sophisticated models. The structures generated in Figures 2−6 took only a few minutes of a Macintosh G3 PowerBook, whereas the simulations shown in Figure 1 took more than 5 days on the DEC Alpha AXP2100/M500. With a suitable modification the present approach would be available in other microgel-forming systems, e.g., formation of microgels via aqueous redox polymerization of *N*-isopropylacrylamide monomer in the presence of a surfactant (e.g., see ref 16). Although the microgel formation in the PVA system starts from the cross-linking of the polymer, the process in which the polymerization and the cross-linking occur at the same time should be a good model in further developing in the present approach.

Acknowledgment. This research was supported in part by grants to E.K. from the Ministry of Education of Japan (#11305066) and the Kyoto University Foundation funding to K.S.S.

Appendix

To mimic the stability of a chemical bond form by cross-linking, we employ an attractive potential of the Yukawa form,

$$\beta U_{pp} = -A \frac{\exp(-yr)}{r} \tag{A1}$$

where $\beta = 1/k_B T$, k_B is the Boltzmann constant, T is the absolute temperature, A is a measure of the strength of interaction, and y is the rate of decay of the interaction with distance of separation r, which is given in units of the radius of the macroion. The characteristics of U_{pp} are such that its influence goes to zero within a reasonable separation distance. To this end, the parameters A and y were arbitrarily chosen to give a very deep but short-ranged attractive potential well when coupled with the infinite repulsion of hard-sphere overlap conditions. Through trial and error the parameters $A = 2.2 \times 10^9$ and $y = 7.34$ were chosen. The profile is shown in Figure 1A, which indicates that the attraction takes place when the particles are within one macroion radius

of each other. The simulations were carried out for several values of the volume fraction, where those simulations reported in this study $\phi_p = 0.01$.

The time evolution of the positional coordinates was achieved by the prescription

$$q_j^{k+1} = q_j^k + \beta D_j \Delta t F_{q_j} + \omega\sqrt{D_j \Delta t} \qquad \text{(A2)}$$

where D_j is the diffusion coefficient, Δt is the time interval for the move, $-1 \le \omega \le +1$ is a random number, and F_j is force exerted on the jth particle by all of the other particles present,

$$F_{q_j} = \sum_{i=1, i\neq j}^{N_p} F_{q_{j,i}} = -\sum_{i=1, i\neq j}^{N_p} \left(\frac{\partial U_{ji}}{\partial q_{j,i}}\right) \qquad \text{(A3)}$$

where U_{ji} is given by eq A1, and the derivative is taken with respect to the qth coordinate distance between the jth and ith particles. In practice, the mean-square displacement along one coordinate is used in the simulations reported herein, where the "step size" s is assumed to be $2D\Delta t = \langle s^2 \rangle$. The step size in these simulations was $s = 0.1$.

The BD simulations were carried out on a DEC Alpha AXP2100/M500 at the University of Missouri Computing Facilities. These results were analyzed and graphically represented using *Mathematica* on a Macintosh G3 PowerBook. The results are shown in Figure 1. Particles with separation distances in the range $2 < r < 3$ are therefore "trapped" as pairs which physically means that a chemical bond is formed. Figure 1B shows the initial configuration of the particles in a cubic array for $\phi_p = 0.01$. Figure 1C is the final configuration after each particle was given 10^7 chances to move. Of course, the aggregated particle cannot move since the Velcro potential is too strong to be overcome by the random movement of the particles. The resulting configurations are highly extended due to the excluded-volume effects. Hence, these simulations justify the inclusion of a "bias" parameter in one direction for the generation of the chains.

References and Notes

(1) Bowman, W. A. Eur. Pat. Appl. 121,141, 1984.
(2) Abel, E. P.; Bowman, W. A. U.S. Pat. 4,404,569, 1985.
(3) Petlon, R. H.; Chibante, P. *Colloids Surf.* **1986**, *20*, 247.
(4) Hirose, Y.; Amiya, T.; Hirokawa, Y.; Tanaka, T. *Macromolecules* **1987**, *20*, 1342.
(5) Matsuo, E. S.; Tanaka, T. *J. Chem. Phys.* **1988**, *89*, 1695.
(6) Pelton, R. H.; Pelton, H. M.; Morphesis, A.; Rowell, R. L. *Langmuir* **1989**, *5*, 816.
(7) Kawaguchi, H.; Fujimoto, K.; Mizuhara, Y. *Colloid Polym. Sci.* **1992**, *270*, 55.
(8) Tam, K. C.; Ragaram, S.; Pelton, R. H. *Langmuir* **1994**, *10*, 418.
(9) Makino, K.; Yamamoto, S.; Fujimoto, K.; Kawaguchi, H.; Ohshima, H. *Colloid Interface Sci.* **1994**, *166*, 251.
(10) Matsumura, Y.; Hyodo, A.; Nose, T.; Ito, S.; Hirano, T.; Ohashi, S. *J. Biomater. Sci., Polym. Ed.* **1996**, *7*, 795.
(11) Weissman, J. M.; Sunkara, H. B.; Tse, A. S.; Asher, R. A. *Science* **1996**, *274*, 959.
(12) Wu, C.; Zhou, S. *Macromolecules* 1**997**, *30*, 574.
(13) Lowe, T. L.; Tenhu, H. *Macromolecules* **1998**, *31*, 1590.
(14) Zhou, S.; Chu, B. *J. Phys. Chem. B* **1998**, *102*, 1364.
(15) Suzuki, H.; Wang, B.; Yoshida, R.; Kokufuta, E. *Langmuir* **1999**, *15*, 4283.
(16) Ito, S.; Ogawa, K.; Suzuki, H.; Wang, B.; Yoshida, R.; Kokufuta, E. *Langmuir* **1999**, *15*, 4289.
(17) (a) Sakurada, I.; Ikada, Y. *Bull. Inst. Chem. Res., Kyoto Univ.* **1966**, *44*, 66. (b) Ikada, Y. *Hoshasen Kobunshi* **1996**, *7*, 3 (in Japanese).
(18) Burchard, W. *Adv. Polym. Sci.* **1983**, *48*, 1. This review paper dealt not only with the theoretical fundamentals of static and dynamic light scattering but also with its application to branched polymers and microgels.
(19) Brasch, U.; Burchard, W. *Macromol. Chem., Phys.* **1996**, *197*, 223.
(20) Wang, B.; Mukataka, S.; Kodama, M.; Kokufuta, E. *Langmuir* **1997**, *13*, 6108.
(21) Wang, B.; Kodama, M.; Mukataka, S.; Kokufuta, E. *Polym. Gels Networks* **1988**, *6*, 71.
(22) See, for example: (a) Peppas, N. A. In *Hydrogels in Medicine and Pharmacy*; CRC Press: Boca Raton, FL, 1987; Vol. II. (b) Mongia, N. K.; Anseth, K. S.; Peppas, N. A. *J. Biomater. Sci., Polym. Ed.* **1996**, *7*, 1055.
(23) Berkowitch, J.; Charlesby, A.; Desreux, V. *J. Polym. Sci.* **1957**, *25*, 490.
(24) Alexander, P.; Charlesby, A. *J. Polym. Sci.* **1957**, *23*, 355.
(25) Danno, A. *J. Phys. Soc. Jpn.* **1958**, *13*, 722.
(26) Matsumoto, A. *Kobunshi Kagaku* **1963**, *20*, 275 (in Japanese).
(27) Kiran, E.; Rodriguez, F. *J. Macromol. Sci., Phys.* **1973**, *B7*, 209.
(28) Ikada, Y.; Mita, T.; Sakurada, I.; Hatada, M. *Radiat. Phys. Chem.* **1977**, *9*, 633.
(29) Chen, W.; Bao, H.; Zhang, M. *Radiat. Phys. Chem.* **1985**, *26*, 43.
(30) Lubis, R.; Olejniczak, J.; Rosiak, J.; Kroh, J. *Radiat. Phys. Chem.* **1990**, *36*, 249.
(31) Ulanski, P.; Bothe, E.; Rosiak, J. M.; Sonntag, C. *Macromol. Chem., Phys.* **1994**, *195*, 1443.
(32) von Sonntag, C.; Bothe, E.; Ulanski, P.; Deeble, D. J. *Radiat. Phys. Chem.* **1995**, *46*, 527.
(33) Kirkwood, J. G. *J. Polym. Sci.* **1954**, *12*, 11.
(34) Bloomfield, V. A.; Van Holde, K. E.; Dalton, W. O. *Biopolymers* **1967**, *5*, 149.
(35) Garcia de la Torre, J.; Bloomfield, V. A. *Biopolymers* **1977**, *16*, 1747.
(36) Garcia de la Torre, J.; Bloomfield, V. A. *Q. Rev. Biophys.* **1981**, *14*, 1.
(37) Zimm, B. H. *Macromolecules* **1980**, *13*, 592.
(38) Zimm, B. H. *Macromolecules* **1984**, *17*, 795.

MA010956+